

AD-A107 034

NAVAL RESEARCH LAB WASHINGTON DC  
ATMOSPHERIC TURBULENCE AS A FUNCTION OF HEIGHT ABOVE VARIOUS SU--ETC(U)  
SEP 81 D H GARCIA  
NRL-8518

F/G 20/4

UNCLASSIFIED

NL

1 of 1  
AD  
81 7044



END  
DATE  
FILMED  
12-81  
DTIC

**LEVEL** ~~///~~

✓ **NRL Report 8518**

AD A107034

# **Atmospheric Turbulence as a Function of Height Above Various Surface Materials**

②

**DANIEL H. GARCIA**

*Optical Radiation Branch  
Optical Sciences Division*

September 23, 1981

NOV 10 1981  
H



**NAVAL RESEARCH LABORATORY**  
Washington, D.C.

Approved for public release; distribution unlimited.

**81 11 06004**

**DTC FILE COPY**

Tu  
X

UNCLASSIFIED

SECURITY CLASSIFICATION OF THIS PAGE (When Data Entered)

REPORT DOCUMENTATION PAGE		READ INSTRUCTIONS BEFORE COMPLETING FORM
1. REPORT NUMBER NRL Report 8518	2. GOVT ACCESSION NO. AD-A107 034	3. RECIPIENT'S CATALOG NUMBER 9
4. TITLE (and Subtitle) ATMOSPHERIC TURBULENCE AS A FUNCTION OF HEIGHT ABOVE VARIOUS SURFACE MATERIALS		5. TYPE OF REPORT & PERIOD COVERED Interim report Continuing NRI Problem.
7. AUTHOR(s) Daniel H. Garcia		6. PERFORMING ORG. REPORT NUMBER
9. PERFORMING ORGANIZATION NAME AND ADDRESS Naval Research Laboratory Washington, DC 20375		8. CONTRACT OR GRANT NUMBER(s)
11. CONTROLLING OFFICE NAME AND ADDRESS Naval Sea Systems Command PM-22/PMS-405 Washington, DC 20362		10. PROGRAM ELEMENT, PROJECT, TASK AREA & WORK UNIT NUMBERS NRL Problem R05-31 Program Element G3754N Project S0182A
14. MONITORING AGENCY NAME & ADDRESS (if different from Controlling Office)		12. REPORT DATE September 23, 1981
		13. NUMBER OF PAGES 22
		15. SECURITY CLASS. (of this report) UNCLASSIFIED
		15a. DECLASSIFICATION/DOWNGRADING SCHEDULE
16. DISTRIBUTION STATEMENT (of this Report)  Approved for public release; distribution unlimited.		
17. DISTRIBUTION STATEMENT (of the abstract entered in Block 20, if different from Report)		
18. SUPPLEMENTARY NOTES		
19. KEY WORDS (Continue on reverse side if necessary and identify by block number)  Atmospheric turbulence Optical propagation		
20. ABSTRACT (Continue on reverse side if necessary and identify by block number) The atmospheric refractive-index structure parameter $C_n^2$ was determined at heights 0.5 to 5 meters above open-field grass, blacktop, concrete, and aluminized-Mylar sheets attached to plywood. Measurements were made of the temperature structure parameter $C_t^2$ with twin fast-response, temperature-sensing probes [R. W. Harris, NRL Report 7587, July 1973] made of 2- $\mu$ m-diameter platinum wire which were separated 10 cm and optimally excited at 10 $\mu$ W. The RMS value of the temperature difference between the probes was determined with an R. W. Harris double-AC-bridge/log-meter system. Probe height was changed approximately every 30 minutes. The differential temperature (Continued)		

DD FORM 1 JAN 73 1473

EDITION OF 1 NOV 65 IS OBSOLETE  
S/N 0102-014-6601

SECURITY CLASSIFICATION OF THIS PAGE (When Data Entered)

20. ABSTRACT (Continued)

and the meteorological parameters comprising air temperature, dew point, wind speed and direction, solar insolation, and barometric pressure were sampled at 1-second intervals. Results indicate a height dependence of the form  $C_h^2 = KH^{-M}$ , where K is a function of the surface ( $0.84 \leq K/10^{-13} \text{ m}^{-2/3} \leq 1.8$ ) and  $M = -1.2 \pm 0.5$ , with the wide variation in M due to changing meteorological conditions, most importantly solar insolation and wind speed. In this experiment, no significant differences in average value of  $C_h^2$  could be determined for the four surfaces. Additionally, the anticipated reduction in turbulence over aluminized Mylar was not observed.

*in ... 2/ = ...*  
*...*

*...*

## CONTENTS

INTRODUCTION .....	1
EXPERIMENT AREAS AND EQUIPMENT .....	2
Sites and Surfaces .....	2
Mobile Tower, Meteorological Sensors, and $C_7$ Probes .....	2
EXPERIMENTAL PROCEDURE .....	7
RESULTS .....	8
$C_n^2$ Over Grass .....	8
$C_n^2$ Over Blacktop .....	12
$C_n^2$ Over Concrete .....	12
$C_n^2$ Over Aluminized Mylar .....	14
Overnight Measurements of $C_n^2$ Over Aluminized Mylar at 3.0 m .....	17
CONCLUSIONS .....	17
RECOMMENDATIONS .....	18
ACKNOWLEDGMENTS .....	18
REFERENCES .....	18

Accession For	
NTIS GRA&I	<input checked="checked" type="checkbox"/>
DTIC TAB	<input type="checkbox"/>
Unannounced	<input type="checkbox"/>
Justification	
By _____	
Distribution/	
Availability Codes	
Avail and/or	
Special	

A

# ATMOSPHERIC TURBULENCE AS A FUNCTION OF HEIGHT ABOVE VARIOUS SURFACE MATERIALS

## INTRODUCTION

This report presents the results of an experiment designed to determine the turbulence strength over four surfaces having differing reflective and physical properties. The objective is to use these results in selecting a method of treating surfaces near a high-energy laser beam which yields minimum thermally induced turbulence and reduced optical degradation of the high-powered beam.

Light waves propagating through the atmosphere exhibit random fluctuations in amplitude and phase due to variations in the index of refraction along the path. An example of this is starlight scintillation. Refractive-index variations are directly related to pressure, temperature, and humidity inhomogeneities resulting from turbulent motion in a real atmosphere, with the turbulent motion being due to changes in net radiative flux, wind speed and direction, and surface roughness. Much theoretical and experimental work has been performed to attempt an understanding of propagation through turbulent regimes. Specifically, the efforts of Kolmogorov [1], Obukov [2], Chernov [3], and Tatarskii [4,5] should be mentioned; much of the theory required for understanding the research documented in this report is found in these references.

The inhomogeneities produced by atmospheric turbulence are characterized by an inner turbulence scale  $l_0$ , representing the smallest eddy size that can be sustained against viscous losses, and an outer turbulence scale  $L_0$ , representing large-scale effects resulting from wind velocity, wind shear, height above the ground or water, and the like. The inner scale is usually about 1 to 10 mm, depending on turbulence strength: the more developed the turbulence, the smaller the inner turbulence scale. The outer turbulence scale can be about 1 to 10 m and represents the largest scale for which turbulence is homogeneous and isotropic.

The random variations in the index of refraction can be described by a structure function:

$$D_n(\mathbf{r}) = \overline{[n(\mathbf{x}) - n(\mathbf{x} + \mathbf{r})]^2}, \quad (1)$$

where  $\mathbf{r}$  is the displacement between two points in space. A similar structure function can be defined for temperature:

$$D_T(\mathbf{r}) = \overline{[T(\mathbf{x}) - T(\mathbf{x} + \mathbf{r})]^2}. \quad (2)$$

Under the assumption of locally isotropic and homogeneous turbulence, Kolmogorov derived a structure function in a form now commonly referred to as the two-thirds law:

$$D_n(r) = C_n^2 r^{2/3} \quad (3)$$

and

$$D_T(r) = C_T^2 r^{2/3}, \quad (4)$$

where  $l_0 < r = |\mathbf{r}| < L_0$  and where  $C_n$  and  $C_T$  are respectively the structure-function parameters for refractive index and temperature. From Eqs. (3) and (4) one can see that the turbulence strength is reflected in the value of  $C_n^2$  or  $C_T^2$ . The structure-function parameters are related by the expression [6]

$$C_n = \frac{77.6P}{T^2} \left[ 1 + \frac{0.00753}{\lambda^2} \right] 10^{-6} C_T. \quad (5)$$

where  $P$  is the pressure in millibars,  $T$  is the temperature in kelvins, and  $\lambda$  is the wavelength in micrometers. For visible wavelengths, such as those of a 0.633- $\mu$ m He-Ne laser, Eq. (5) becomes

$$C_n = \frac{79P}{T^2} 10^{-6} C_T, \quad (6)$$

the form usually seen in the literature [7]. By combining Eqs. (2) and (4) and substituting the resulting expression for  $C_T$  into Eq. (6), one arrives at an equation relating variations in index of refraction to a temperature differential:

$$C_n = \frac{79P}{T^2} 10^{-6} \frac{[(T_1 - T_2)^2]^{1/2}}{r^{1/3}}, \quad (7)$$

where  $T_1$  and  $T_2$  are the temperatures at two points separated a distance  $r$ . Equation (7) will be used to determine  $C_n^2$  from measurements of the RMS value of the temperature difference  $\Delta T$  between two fine-wire fast-response thermal probes, as has been done previously [6,8,9].

The structure parameter  $C_n^2$  can also be determined from optical scintillation measurements [9]; however, this measurement requires double-ended experiments over paths 100 m long if reasonable signal-to-noise ratios are to be obtained. For the present work, the availability of a mobile thermal-probe system and the requirement to study several different surface materials indicated that deriving  $C_n^2$  from measurements of  $\Delta T$  would be more feasible in a limited time frame and much less expensive than the use of optical scintillation techniques.

## EXPERIMENT AREAS AND EQUIPMENT

### Sites and Surfaces

During October and November 1977, measurements were made of  $C_T$  over open-field grass, blacktop, concrete, and aluminized Mylar at the Chesapeake Bay Detachment (CBD) of NRL. The open-field grass comprises a relatively extensive area of open meadow with gradual slopes in what is called West Field. Measurements over the other three surfaces were performed next to Building 49 in another section of CBD, somewhat closer to buildings and trees. This second experimental site contained blacktop and concrete areas. In addition, 32 sheets of 4-by-8-ft plywood, covered with aluminized Mylar and stapled on the underside, were placed on the concrete area to make a 95-m<sup>2</sup> (1024-ft<sup>2</sup>) extended square area, as shown in Fig. 1. Figure 2 provides the dimensions of the blacktop and concrete areas and shows the location of the trailer van which housed the data-acquisition system and the electronics for the meteorological sensors and thermal probes.

### Mobile Tower, Meteorological Sensors, and $C_T$ Probes

Figures 3 and 4 show the mobile tower on which sensors were mounted for monitoring air temperature, dew point, wind speed, and wind direction. Also shown in Fig. 4 are the fast-response thermal probes used for measuring  $C_T$  and the radiometer used for determining global radiation.

Air temperature and dew point were monitored with an EG&G model 110S-M automatic dew-point hygrometer having a range of -62°C to 49°C, a response time of 1.7°C/s, and an accuracy of 0.3°C. Wind speed and direction were obtained from an R. M. Young Company model 35003 Gill propeller vane having a wind-speed threshold of 0.1 to 0.2 m/s and a range of 0 to 30 m/s. Global radiation, the sum of direct solar radiation and diffuse atmospheric radiation, was measured using an Eppley Laboratory thermopile pyranometer having a response time of 3 to 4 s and an output of 11.25  $\mu$ V per W/m<sup>2</sup>. Barometric pressure was monitored with a Yellow Springs Instrument Company Model 2014 pressure transducer having a range of 833 to 1067 millibars; this sensor was located inside the trailer van.

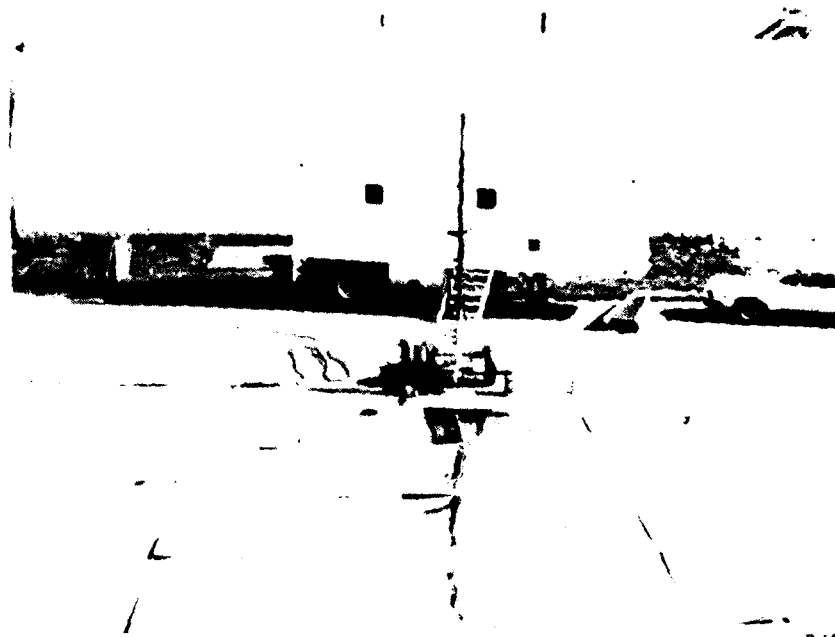


Fig 1 - Mobile tower with meteorological sensors deployed above aluminized-Mylar-covered plywood sheets

R-141

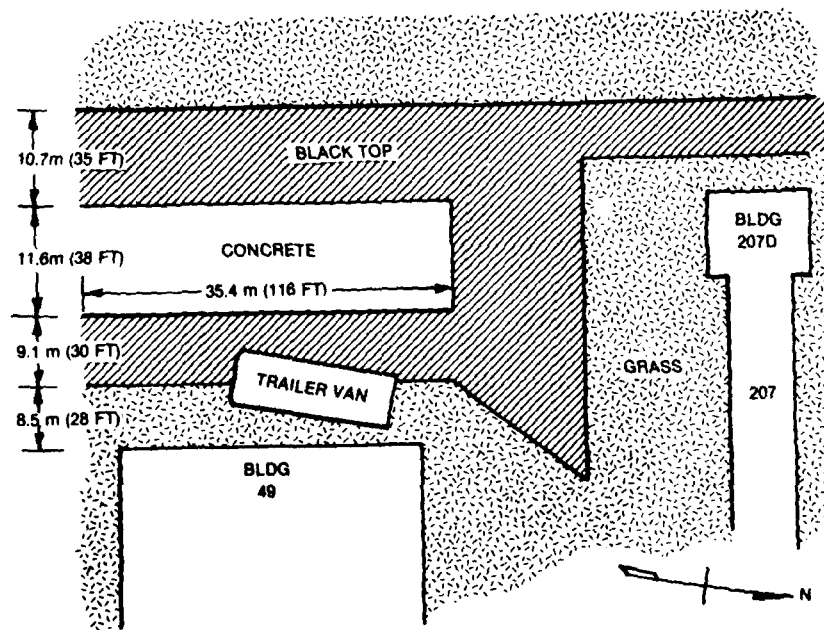
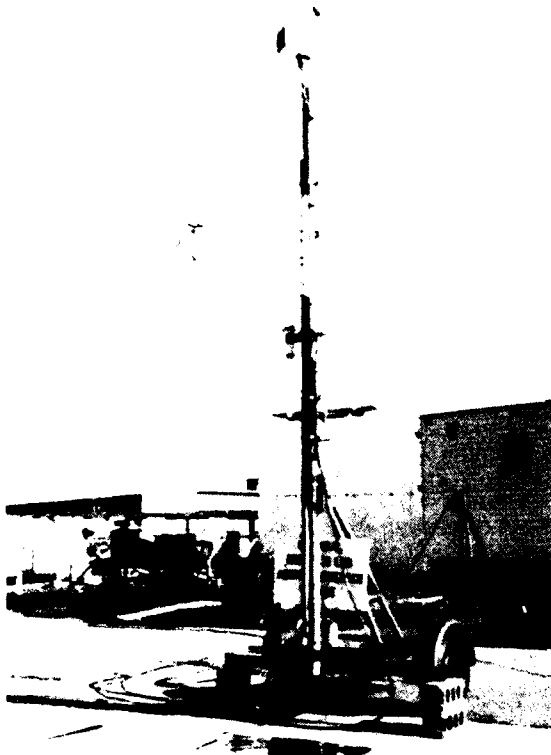


Fig 2 - Layout of concrete and blacktop surfaces available for turbulence measurements

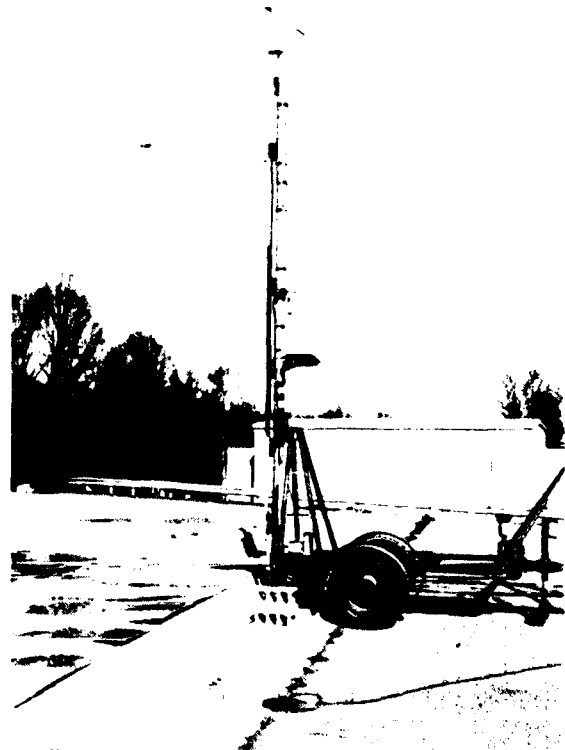




R-136

Fig. 3 — Mobile tower with sensors for monitoring wind direction, wind speed,  $C_T$ , air temperature, and dew point (front view)

Fig. 4 — Side view of the mobile tower



R-137

Figure 5 shows the upper section of the tower. At the top is the Young wind speed and direction sensor; on the right-hand side of the tower is the EG&G sensor. The left-hand side of the tower shows the welded section of Unistrut which supported the movable aluminum L section. The fast-response thermal probes were attached to this section, which was bolted in place at the desired height. For heights over 3 m the entire tower was tilted to a horizontal position to facilitate moving the  $C_7$  probes to a different level.



Fig. 5 - Upper section of the mobile tower

R 139

The dual fine-wire, fast-response temperature probes used for determining  $C_n^2$  through the measurement of  $C_7$  are shown in Fig. 6. The vane assembly kept the two probes pointed into the wind. Each probe uses platinum wire  $2.032 \mu\text{m}$  in diameter and 1.0 mm in length, with the separation between the two probes being 10 cm. These probes are of the same design as that used by Dowling and Livingston [9]. They are part of an AC bridge which allows measurement of the temperature of each probe. The probes are optimally excited with  $10 \mu\text{W}$  of electrical power in accordance with the results of Harris [10]. The electronics required for the thermal probes are divided into a front-end section positioned near the probe assembly (at the base of the tower) and a back-end section, containing a B&K Instruments model 215 RMS-voltmeter/log-converter, installed in the trailer van. The entire system was originally designed by R. W. Harris; a redesign of the front-end unit and modifications of the back-end unit have been performed by Tower Systems, Inc. Similar fast-response, thermal-probe systems are described in Ref. 8. Figure 7 shows one of the fine-wire probes with the protective cap on and the other with the cap removed.

All of the voltages from the previously described sensors were processed by a Monitor Labs 7200 data logger which was connected to a Digidata 130 Series nine-track, incremental, digital tape recorder. The digital tapes were processed on the Texas Instruments Advanced Scientific Computer at NRL using Fortran computer programs developed for this purpose. Computer plots of the data, presented in a later section, were also obtained. Figure 8 is a diagram of the sensors and data-acquisition system.

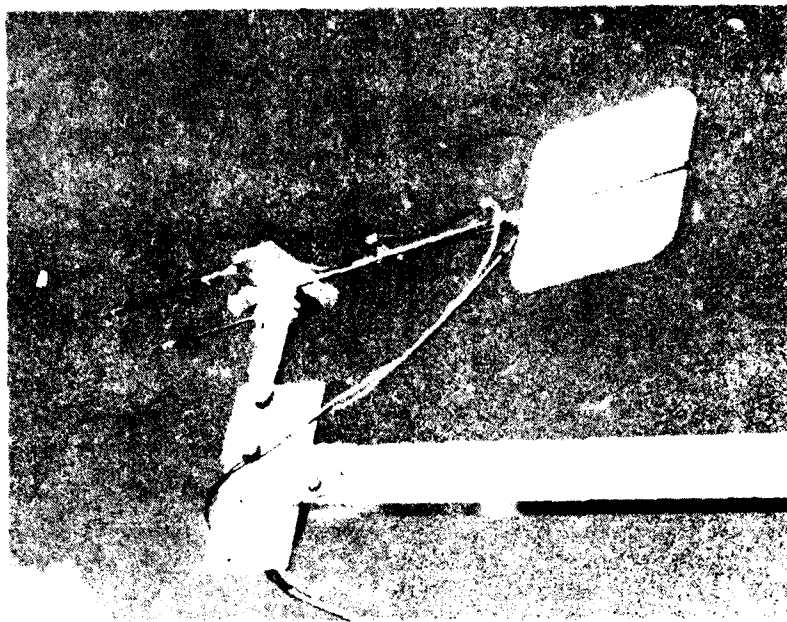


Fig. 6 — Dual fine-wire, fast-response temperature probes for measuring  $C_f$  R-138  
(shown mounted on a wind-vane assembly)

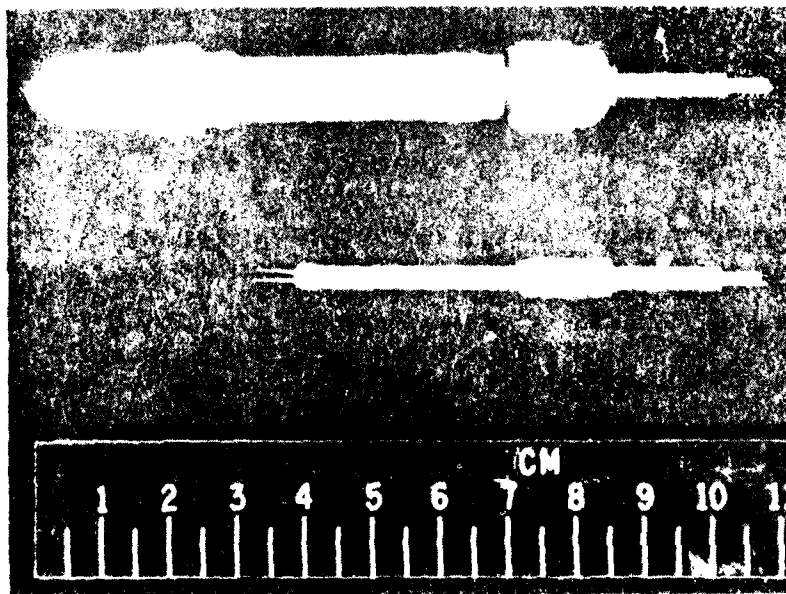


Fig. 7 — Fine-wire thermal probe with the protective cap (top)  
and a probe with the protective cap removed (bottom)

R-140

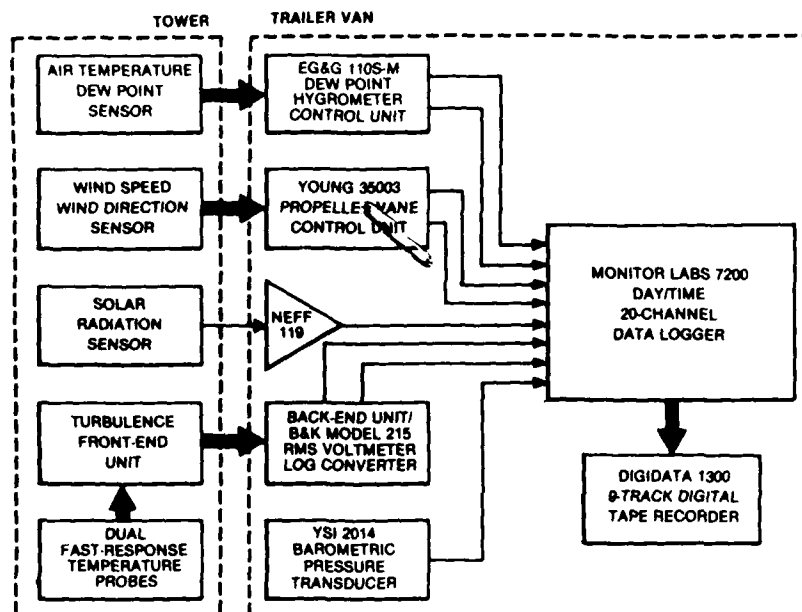


Fig. 8 — Data acquisition system

## EXPERIMENTAL PROCEDURE

Turbulence levels were measured over grass in West Field and over blacktop, concrete, and aluminized Mylar next to Building 49 at CBD. The experimental procedure followed was identical for each of the four surfaces. The mobile tower was placed such that the end where the turbulence probes were located was pointed into the prevailing wind direction to maximize the effect of the surface being studied and minimize the contribution to the turbulence measurement resulting from mechanical mixing of the air surrounding the tower structures. The probes were installed on the vane assembly, the protective caps on each probe were removed, and the protective sheath on each probe was slid back to its farthest position. The exposed probes were left in position overnight, if needed, when weather conditions indicated *no near-term precipitation*, since the platinum-wire structure is relatively sturdy even in high winds. The Eppley radiometer was taken out of the trailer van each day and placed outside next to the tower. The turbulence front-end unit, requiring 117-V AC power, was installed on the tower trailer each day, since this unit was not weatherproof.

All of the meteorological sensors and the data-acquisition systems were activated 1/2 hour prior to the taking of data. The time constant for averaging the temperature difference between the two probes was set to 1 s on the B&K RMS-voltmeter/log-converter. Thus the averaging period of Eq. (6) is the time constant of the B&K instrument. The Monitor Labs data logger scanned all input channels once every second.

Two sizes of computer tape were used: a 183-m (600-ft) reel and a 366-m (1200-ft) reel, depending on the anticipated length of a particular day's run. Each data tape was processed at NRL at the end of the day or on the next day to insure validity of the data and to check on the performance of the sensors and the data-acquisition system.

Measurements of  $C_f$  were made at heights of 0.5, 1, 2, 3, 4, and 5 m above the surface. For the positions from 0.5 to 3 m on the tower, the turbulence probe was moved to the level and bolted in

place; the 4- and 5-m positions required that the tower be tilted to the horizontal before moving the probe assembly to the next position. This latter procedure took approximately 5 to 10 min. Data were taken at each level for intervals ranging from 15 to 45 min. Each minute yielded 60 data points of the meteorological parameters and of  $C_n^2$ ; it was expected that the approximate 1/2-hour data period at each level would suffice for determining  $C_n^2$  for that height above a particular surface.

Data were usually taken during the hours 0900 to 1500. Changes in the weather required shortening the interval during which data were taken, especially when rain was expected or occurred. One run was made from 1630 on 14 November until 0730 the next day to determine the overnight variation of  $C_n^2$  at a level of 3 m over an aluminized-Mylar surface.

For measurements over blacktop (Fig. 2) the mobile tower was placed at the northwest corner of the concrete area with the probes pointed into a northwesterly wind. The measurements over the rectangular concrete area (Fig. 2) were made with the mobile tower at the center with the probes pointed into a westerly wind.

The 32 plywood sheets covered with aluminized Mylar were placed in front of the mobile tower each morning and then taken up, covered, and stored in Building 49 each evening (except for the one overnight run). Through this procedure the mirrorlike reflectivity of this material was maintained during the experimental period.

## RESULTS

### $C_n^2$ Over Grass

Figures 9, 10, 11, and 13 are each a computer plot of the refractive-index structure parameter  $C_n^2$  (denoted (NSQ)), solar radiation, and wind speed versus time of day derived from measurements over grass. The refractive-index structure parameter is plotted on a logarithmic scale as a solid line. Solar radiation, which includes all solar-derived radiation (previously defined as global radiation), is plotted on a linear scale as a dotted line. Wind speed is similarly plotted on a linear scale as a dashed line. The data points plotted are 3-min averages, which in most instances represent the average of 180 measurements obtained using the 1-s scan period of the data logger.

The measurements made on 12 October 1977, are shown in Fig. 9. The skies were overcast, and the wind was out of the northwest at about 2 to 5 m/s, as shown by the dashed curve. The dotted solar-radiation line showed a general increase during the day; the variations are manifestations of the changing cloud cover.

The two vertical bars above the axis show the last data points for the 1.3-m and 3.7-m heights at which the  $C_n^2$  measurements were made. The value of  $C_n^2$ , shown by the solid line, was influenced continuously by the nature of the surface, by the solar radiation, and by the wind speed in a complex interactive process. It is this aspect which makes analysis difficult and comparisons between days subject to varying interpretation. The following comments on the data therefore will tend to be more qualitative than quantitative.

Figure 9 shows three important effects: the influence of wind speed on  $C_n^2$ , the close relationship between  $C_n^2$  and solar radiation, and the decrease in turbulence at greater heights. The first of these effects is seen at 1227. From 1224 to 1230 the solar radiation was approximately constant at  $0.65 \text{ W/m}^2$ , and the height  $H$  above the grass was 3.7 m. Thus two of the important influences on  $C_n^2$  were essentially constant. The distinct peak in wind speed produced an equally distinct trough in  $C_n^2$ , leading to the conclusion that increased wind speed causes decreased small-scale turbulence through the injection of relatively homogeneous masses of air into the measurement region.

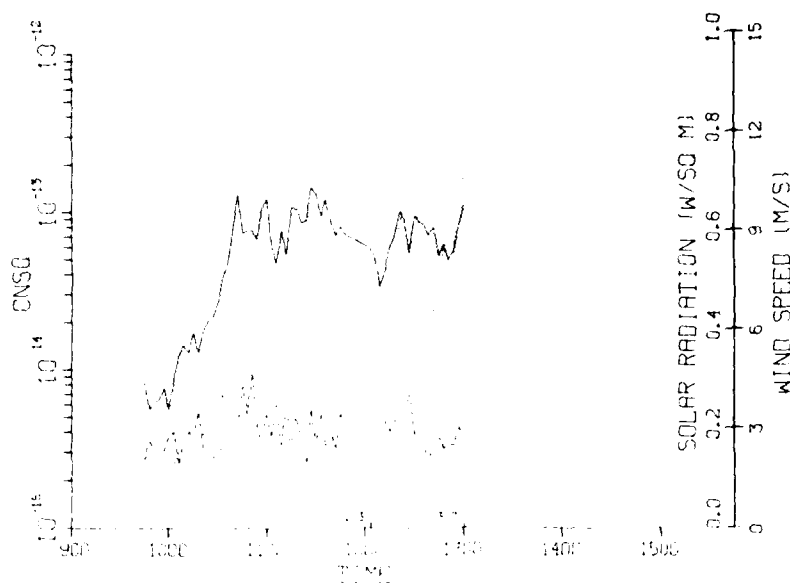


Fig. 9 —  $C_n^2$  above grass (solid line), solar radiation (dotted line) and wind speed (dashed line) on 12 October 1977

The second important effect is seen throughout the day: peaks in the  $C_n^2$  curve correlate with peaks in the solar radiation curve, and troughs in  $C_n^2$  correlate with troughs in solar radiation. Examples of this occur at 1042 (peaks in  $C_n^2$  and solar radiation) and at 1051, 1106, 1121 and 1209 (troughs). If one notes that from 1030 to 1145 the solar radiation has an average value of  $0.4 \text{ W/m}^2$ , one can estimate the influence of solar radiation on the structure parameter: the drop to  $0.27 \text{ W/m}^2$  in solar radiation induces a drop in  $C_n^2$  from its nominal value of  $8 \times 10^{-14}$  to  $5 \times 10^{-14} \text{ m}^{-2/3}$ , a drop of almost 50%. In conjunction with this correlation of solar radiation and  $C_n^2$ , one should note that changes in the structure constant occur with a time lag of about 3 to 6 min, in contrast to the time lag for the influence of the wind speed, which seemed to be imperceptible with the 3-min resolution of the data points.

Finally, the effect of moving the probe to a different height can be observed: At 1203 the probe assembly was moved from a height  $H = 1.3 \text{ m}$  (4 ft) to  $H = 3.7 \text{ m}$  (12 ft), a factor-of-three increase. Between 1209 and 1300 the value of  $C_n^2$  has a slightly lower average of  $7 \times 10^{-14} \text{ m}^{-2/3}$ , even though the solar radiation has a net increase of  $0.2 \text{ W/m}^2$  per hour. This observation implies that the effect of solar radiation on  $C_n^2$  is lessened at heights above 3 m and, most importantly, that tripling the height above a grass surface essentially counteracts the increase in  $C_n^2$  that would occur with the increase of solar radiation from an average  $0.4 \text{ W/m}^2$  to  $0.6 \text{ W/m}^2$  between the heights 1.3 and 3.7 m, a 50% increase in solar radiation. Had the solar radiation remained constant during the measurements at these two heights, one would expect that  $C_n^2$  would be lower. This agrees with Wyngaard et al. [7], whose own data agree with an  $H^{-4/3}$  dependence of  $C_n^2$  for local free convection on a summer day with light winds at heights a few meters above the ground, an experimental situation similar to the one of this report, except for the overcast conditions. To eliminate the effects of changing wind speed and solar radiation, multiple probe assemblies at several heights would be required to deduce the functional dependence of  $C_n^2$  on  $H$ . (The use of the one available probe system made it more difficult to determine an experimental value for the exponent of  $H$ .)

Figure 10 shows the results of the measurements on 17 October 1977, at heights of 0.5, 1.0, and 2.0 m. The day was one of high winds, from 7 to 14 m/s, and clear skies. The inverse relationship

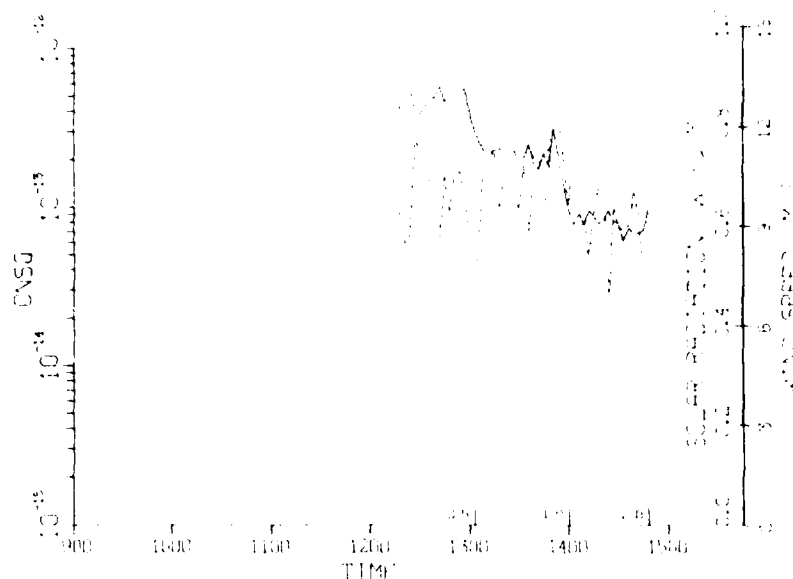


Fig. 10 —  $C_n^2$  above grass (solid line), solar radiation (dotted line), and wind speed (dashed line) on 17 October 1977

between  $C_n^2$  and wind speed is again evident at 1221, 1242, 1336, 1412, 1418, 1424, and 1447, though an increase in  $C_n^2$  to  $3 \times 10^{-13} \text{ m}^{-2/3}$  at 1351 seems to have been caused by an increase in wind speed to a very high 13.7 m/s, an effect opposite to what had been usually observed.

From 1215 until 1400 the solar radiation dropped very little and was essentially  $0.75 \text{ W/m}^2$ ; during this time the winds were gusty, with an average value of 10 m/s. For  $H = 0.5 \text{ m}$ ,  $C_n^2 = 4.5 \times 10^{-13} \text{ m}^{-2/3}$ ; for  $H = 1.0 \text{ m}$ ,  $C_n^2 = 1.9 \times 10^{-13} \text{ m}^{-2/3}$ ; for  $H = 2.0 \text{ m}$ ,  $C_n^2 = 0.9 \times 10^{-13} \text{ m}^{-2/3}$ . By plotting these three data points on a log-log format, one can obtain the relationship between  $C_n^2$  and height  $H$  above the grass on this day:  $C_n^2 = 1.9 \times 10^{-13} H^{-1.16 \pm 0.08} \text{ m}^{-2/3}$ . The theory for unstable free convection with no wind shear indicates an  $H^{-4/3}$  dependence; stable conditions indicate an  $H^{-2/3}$  dependence. Thus the experimentally determined exponent  $-1.16 \pm 0.08$  falls in the proper range between  $-2/3$  and  $-4/3$ ; that it is closer to  $-4/3$  satisfies the initial assumption of the occurrence of free convection [7]. The drop in solar radiation after 1400, which corresponds to the data for 2.0 m, would tend to decrease the values of  $C_n^2$  during this time; this tends to increase the negative slope on the log-log plot, thus indicating that either the exponent lies in a region close to  $-1$  or no simple exponential relationship of the form derived in the theory can describe what occurs in the region below 2 m.

Figure 11 shows the results of the measurements on 18 October 1977. No solar-radiation data are plotted, because of a malfunction that day. Since the skies were clear, one would expect an increase in solar radiation from 900 to 1200 and a gradual decrease thereafter. The winds were out of the southwest at about  $3 \pm 1.5 \text{ m/s}$ . Figure 12 is a log-log plot of  $C_n^2$  versus height for the data shown in Fig. 11. The line drawn has the form  $C_n^2 = 1.8 \times 10^{-13} H^{-1.72} \text{ m}^{-2/3}$ , determined from a graphical estimate of where the line should be. The power of  $H$  is greater than the  $-4/3$  predicted by free-convection turbulence theory. The influence of solar radiation is most apparent for the 0.5-m data (Fig. 12), for which decreased sunlight produced a value of  $C_n^2$  lying below the line.

Figure 13 shows the measurement results for 19 October 1977, at heights of 0.5, 1.0, and 2.0 m. The respective average values of  $C_n^2$  at these heights are  $1.5 \times 10^{-13}$ ,  $0.8 \times 10^{-13}$ , and  $0.5 \times 10^{-13} \text{ m}^{-2/3}$ ; these yield the relation  $C_n^2 = 8.4 \times 10^{-14} H^{-0.81} \text{ m}^{-2/3}$ , which has a power of  $H$  quite different

Fig. 11 —  $C_n^2$  above grass (solid line), and wind speed (dashed line) on 18 October 1977

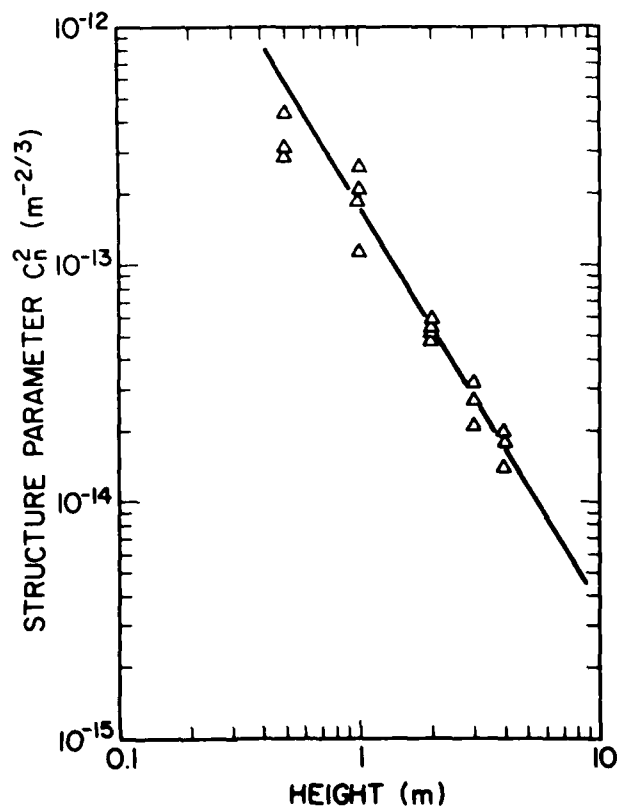


Fig. 12 — Dependence of  $C_n^2$  (above grass) on height for 18 October 1977



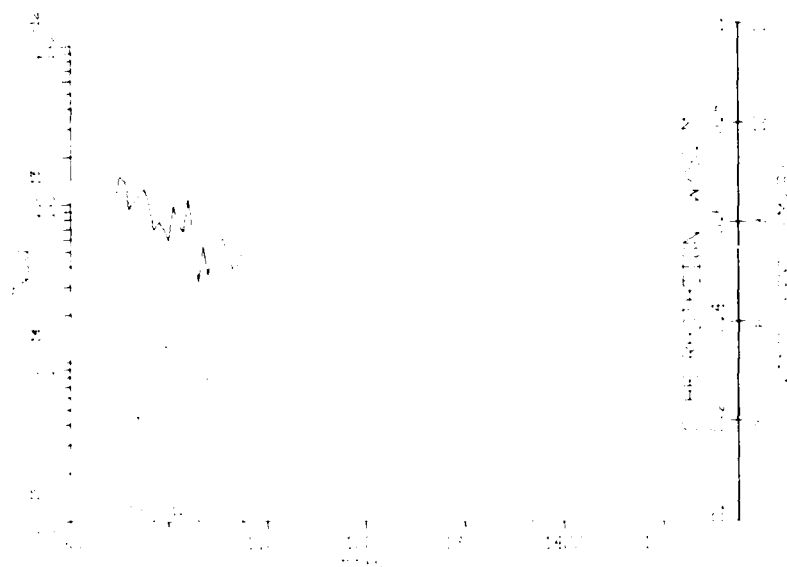


Fig. 13 —  $C_n^2$  above grass (solid line), solar radiation (dotted line), and wind speed (dashed line) on 19 October 1977.

from that obtained on the previous day. However, the rapid increase in solar radiation during the measurement interval ( $0.22 \text{ W/m}^2$  per hour) results in large  $C_n^2$  values for 1.0 and 2.0 m when compared with the case of constant solar radiation. This changing solar radiation does not allow an unambiguous determination of the variation of  $C_n^2$  with height for these data.

#### $C_n^2$ Over Blacktop

Measurements of  $C_n^2$  were made over blacktop on 20 October 1977. The results are presented in Fig. 14. The three effects noted over grass can be seen again: First, at 1012 and 1218 the dip in wind speed produces a concomitant peak in  $C_n^2$ , even though these times correspond to the disparate 5.5- and 1.0-m heights. Second, the large drop in solar radiation occurring at 1306 is paralleled by a significant drop in  $C_n^2$ . Finally, as the measurement height above the blacktop decreased, the value of the structure parameter increased. For 1.0-, 2.0-, and 4.0-m heights, the respective average values of  $C_n^2$  are  $1.2 \times 10^{-13}$ ,  $4.2 \times 10^{-14}$ , and  $2.0 \times 10^{-14} \text{ m}^{-2/3}$ ; a log-log plot of these data yields  $C_n^2 = 1.2 \times 10^{-13} H^{-1.32} \text{ m}^{-2/3}$ , which generally has the same constant and power of  $H$  as previously found in measurements over grass. It is surprising, however, to find that  $H$  has this nearly  $-4/3$  exponent even though the solar radiation increased throughout most of the measurement period. If the same reasoning is used here as was used for the October 19 grass measurements, compensation for the effect of increasing solar radiation would lessen the values of  $C_n^2$  at 2.0 and 1.0 relative to that at 4.0, thus decreasing the power of  $H$ , that is, yielding a value closer to 1.0. This implies that turbulence above blacktop tends to decrease less rapidly with height than it does over grass, which might be expected for a surface which absorbs more solar energy and becomes hotter.

#### $C_n^2$ Over Concrete

Measurements were made on 31 October 1977, over concrete, and the results are shown in Fig. 15. Approximate average values of  $C_n^2$  at 0.5, 1.0, 2.0, 3.0, 4.0, and 5.0 m are respectively 3.2, 2.0, 4.5, 3.0, 2.3, and  $2.0 \times 10^{-14} \text{ m}^{-2/3}$ . The day became cloudy at around 1330, at which time solar radiation and wind speed fell rapidly; measurements at 1.0 m were ongoing during this change in conditions.

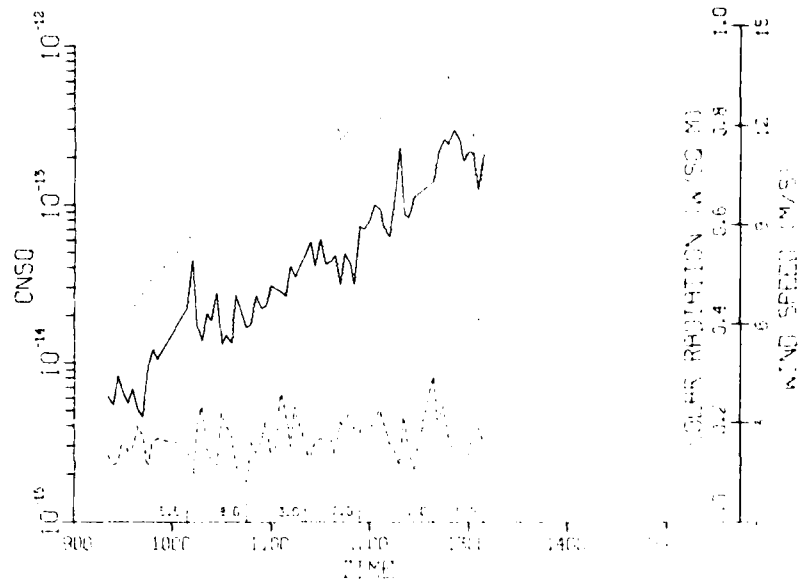


Fig. 14 —  $C_n^2$  above blacktop (solid line), solar radiation (dotted line), and wind speed (dashed line) on 20 October 1977

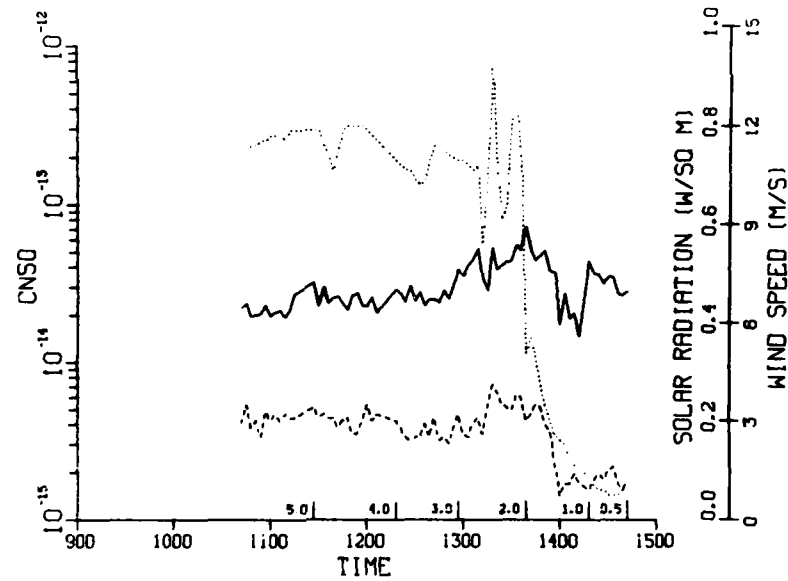


Fig. 15 —  $C_n^2$  above concrete (solid line), solar radiation (dotted line), and wind speed (dashed line), on 31 October 1977

The  $C_n^2$  values for 0.5 and 1.0 m are approximately an order of magnitude lower than they would have been had the solar radiation remained at  $0.75 \pm 0.05 \text{ W/m}^2$ , that for 2.0 to 5.0 m. The changes in weather conditions essentially change the multiplicative constant in the  $C_n^2$  equation. The data lead to two equations:

$$C_n^2 = 2.0 \times 10^{-14} H^{-0.68} m^{-2/3}, \quad H = 0.5, 1.0 \text{ m};$$

and

$$C_n^2 = 9.0 \times 10^{-14} H^{-1.0} m^{-2/3}, \quad H = 2.0 \text{ to } 5.0 \text{ m}.$$

These two equations are derived from Fig. 15; the values of  $C_n^2$  at the lower heights are small, thus leading to large differences in the structure constant at these levels, with a resulting greater uncertainty in the exponent of  $H$ . Figure 15 at first would seem to indicate lower  $C_n^2$  values for concrete than for blacktop (Fig. 14). However, for the blacktop data the solar radiation was increasing during most of the measurements, whereas for the concrete the solar radiation was essentially unchanged for  $H$  above 3.0 m. The two previous equations for  $C_n^2$  actually give values for the structured constant which are larger than those calculated from the blacktop  $C_n^2$  equation. The intuitive concept that turbulence levels above concrete, which tends to reflect more solar radiation, should be less than those over blacktop thus is not verified. Perhaps this is due to the uncertainties in the data for concrete; a more likely explanation is that the experimental concrete area was rather small and also surrounded on three sides by blacktop, with turbulence over the blacktop influencing the turbulence over the concrete.

### $C_n^2$ Over Aluminized Mylar

Figures 16 through 19 show the results of measurements made over an aluminized-Mylar surface. The data for 1 November 1977, shown in Fig. 16 were obtained using only 12 of the 32 sheets of aluminized-Mylar-covered plywood. The solar radiation increased from 0951 to 1115 and decreased thereafter due to the increasing cloud cover. The effect of broken cloud cover prior to 1130 is evident. The winds remained at about 3 m/s. The variations in solar radiation make it difficult to extract quantitative changes in  $C_n^2$  at the various heights, though the drop in turbulence with increasing height is apparent.

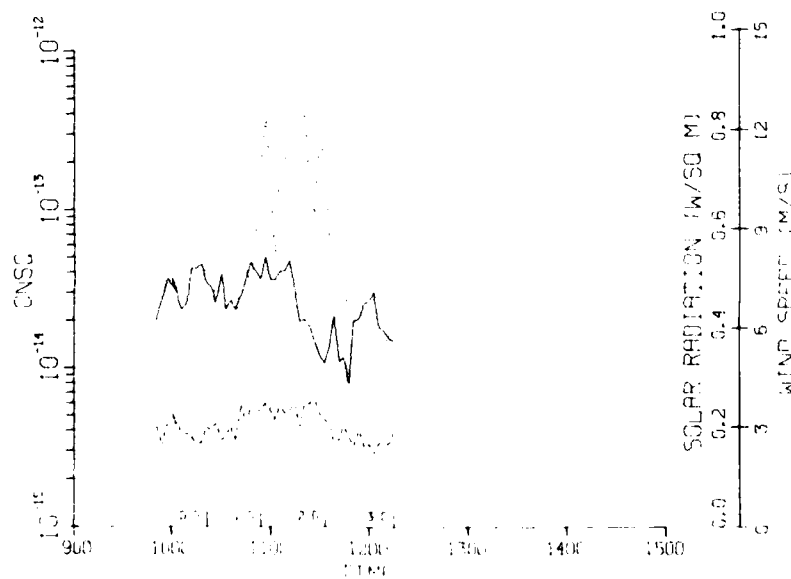


Fig 16 -  $C_n^2$  above aluminized Mylar (solid line), solar radiation (dotted line), and wind speed (dashed line) on 1 November 1977

Figure 17 shows the results for 11 November 1977, a day beset by broken clouds with winds  $2 \pm 1$  m/s out of the west to southwest. The broken cloud cover produced wide variations in solar radiation which led to large changes in  $C_n^2$ ; the effect is clearly evident at 1103, 1148, 1212, 1233, and 1336 (peaks) and at 1142, 1203, 1318, and 1354 (troughs). Because of these many variations in solar radiation, it is again difficult to determine quantitatively the height dependence of  $C_n^2$ ; however, the general tendency to increased  $C_n^2$  with decreased height is again apparent. More importantly, this figure shows that aluminized Mylar produces turbulence levels which have a wider response to solar radiation, ranging from  $5.25 \times 10^{-15} \text{ m}^{-2/3}$  at 1142 to  $3.44 \times 10^{-13} \text{ m}^{-2/3}$  at 1412.

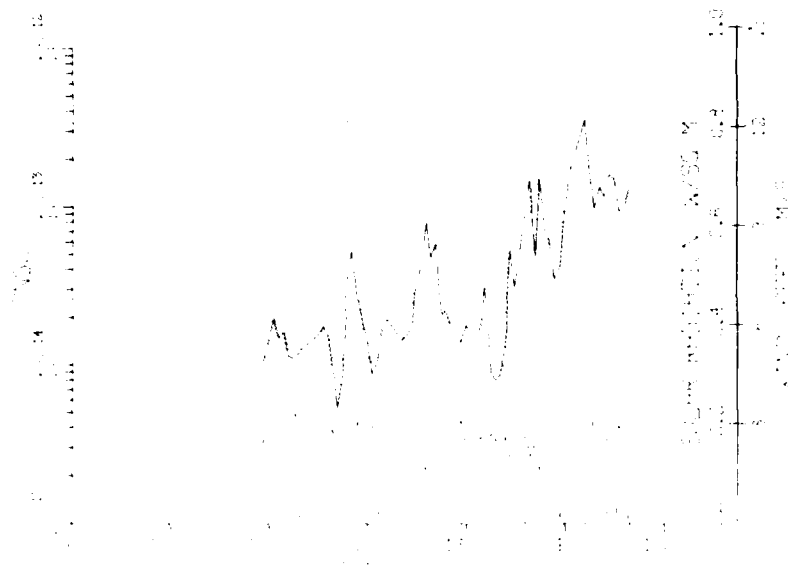


Fig. 17 -  $C_n^2$  above aluminized Mylar (solid line), solar radiation (dotted line), and wind speed (dashed line) on 11 November 1977

Figure 18 shows the results of data taken on 14 November 1977. Some clouds caused variations in the solar radiation during the measurement period. The direct relation between  $C_n^2$  and solar radiation is evident in the troughs at 1009, 1036, 1124, 1200, and 1218 and in the peaks at 1151, 1209, and 1224. Estimated average  $C_n^2$  values at 0.5, 1.0, and 2.0 m are respectively  $2.8$ ,  $1.4$  and  $0.86 \times 10^{-13} \text{ m}^{-2/3}$ , which lead to  $C_n^2 = 1.5 \times 10^{-13} H^{0.86} \text{ m}^{-2/3}$ . The influence in the power of  $H$  due to increasing solar radiation is evident; had the solar radiation remained constant, the  $C_n^2$  value at 1.0 and 2.0 m would have been lower, producing a higher value for the exponent of  $H$ , which is in the correct direction and perhaps nearer the 1 to 1.3 obtained for the other surfaces. The larger variation in  $C_n^2$  with change in solar radiation is clearly seen; that is, the turbulence level above aluminized Mylar is more sensitive to solar radiation than it is above grass, concrete, and blacktop.

The results for 18 November 1977, are shown in Fig. 19. The skies were clear until 1100, when some clouds appeared, causing significant drops in solar radiation. The dependence of  $C_n^2$  on solar radiation is especially evident at 1103 and 1203. Values for  $C_n^2$  at 1.0, 2.0, 3.0, 4.0, and 5.0 m are respectively  $18$ ,  $7.5$ ,  $5.0$ ,  $2.8$ , and  $2.3 \times 10^{-14} \text{ m}^{-2/3}$ , which lead to  $C_n^2 = 1.8 \times 10^{-13} H^{-1.3} \text{ m}^{-2/3}$ . This power of  $H$  is in agreement with the theoretical value of  $-4/3$ , but the increase of solar radiation during the measurements would imply a reduction in the  $H$  exponent.

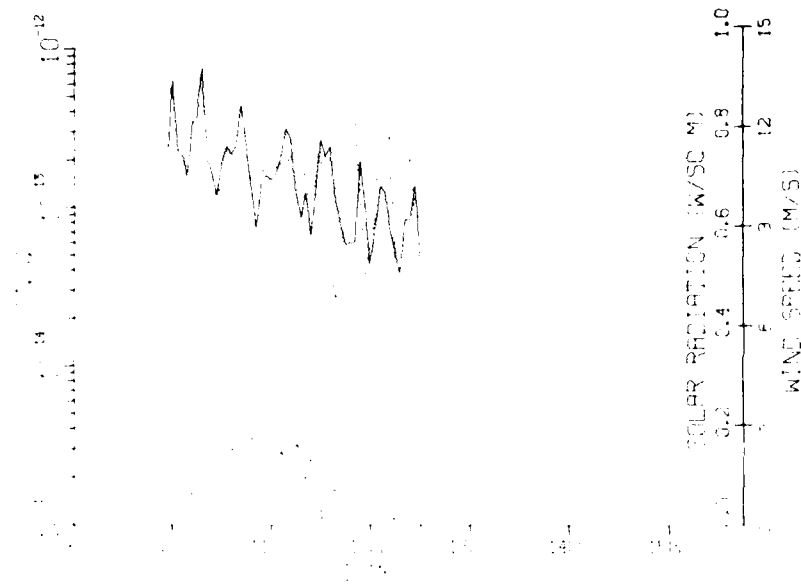


Fig. 18 -  $C_n$  above aluminized Mylar (solid line), solar radiation (dotted line) and wind speed (dashed line) on 14 November 1977

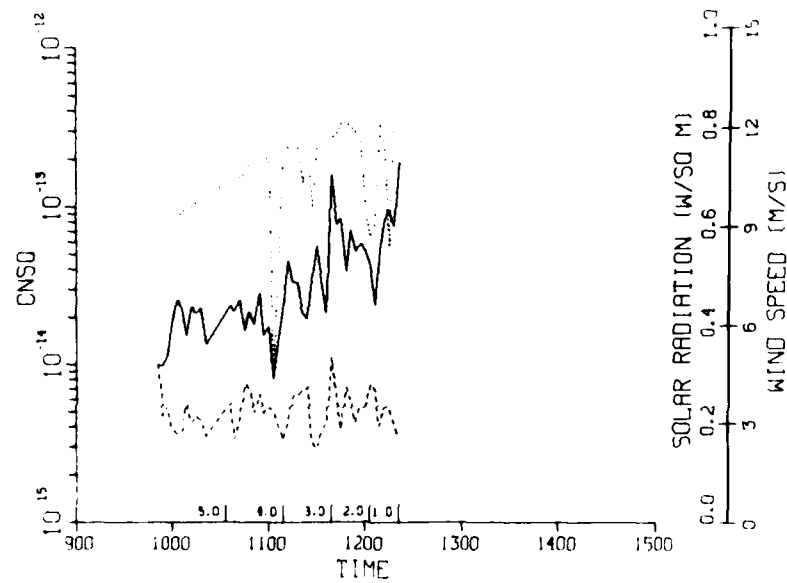


Fig. 19 -  $C_n$  above aluminized Mylar (solid line), solar radiation (dotted line) and wind speed (dashed line) on 18 November 1977

For the four measurement days with aluminized Mylar, it seems that the height dependence of  $C_n^2$  is proportional to a power of  $H$  in the neighborhood of  $-1$ . The influence of solar radiation seems to be greater than for the prior three surfaces. Originally it had been proposed that the specular nature of aluminized Mylar would lead to a lowering of turbulence above this surface. The results of this experiment do not support this hypothesis; they showed an increase in the dynamic range of the turbulence. Again turbulence from bordering surfaces may be significant.

#### Overnight Measurements of $C_n^2$ Over Aluminized Mylar at 3.0 m.

Figure 20 shows the results of measurements made from 1418 on 14 November until 0730 on 15 November 1977, at 3.0 m above aluminized Mylar. The skies were clear during the night, and the winds decreased toward sunset and rose slightly during the night. The logarithmic scale for  $C_n^2$  is compressed by an additional cycle from that of the previous figures due to  $C_n^2$  minima below  $10^{-15} \text{ m}^{-2/3}$ . Important effects that can be seen are the decrease in  $C_n^2$  with decrease in solar radiation, leading to a minimum after sunset, when the air temperature and surface temperature became equal, an increase in  $C_n^2$  during the night, due to the reversal in direction of the net heat flux after sunset and a minimum after sunrise when the air temperature and surface temperature again become equal. The increased wind speed from 0300 to 0500 appears to reduce the turbulence during this time, in accord with the results obtained for the daytime measurements.

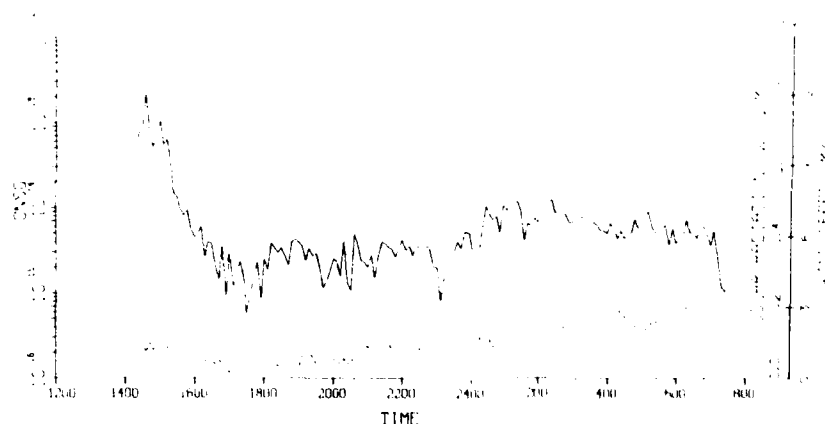


Fig. 20 —  $C_n^2$  above aluminized Mylar (solid line), solar radiation (dotted line), and wind speed (dashed line) on 14 and 15 November 1977

#### CONCLUSIONS

Based on the data shown in Figs. 9 through 20, the following observations can be made:

- The refractive-index structure parameter  $C_n^2$  is inversely related to wind speed at heights up to 5 m over the four surfaces studied.
- $C_n^2$  is a direct function of the solar radiation. There is a stronger correlation for aluminized Mylar than for grass, blacktop, or concrete.
- $C_n^2$  is an inverse function of the height above the surface; the relationship has the form  $C_n^2 = KH^{-M}$ , where  $K$  depends on the type of surface,  $0.84 \leq K/10^{-13} \text{ m}^{-2/3} \leq 1.8$ , and  $M$  varies with surface and meteorological conditions. For this experiment  $0.68 \leq M \leq 1.72$ , with  $M = 1.2$  being a good estimate in most instances.

- No significant difference in the average value of  $C_n^2$  could be determined in this experiment for the four surfaces studied, though the range of the structure parameter was greater for aluminized Mylar. An anticipated reduction in  $C_n^2$  over the aluminized-Mylar surface was not observed in this experiment.

## RECOMMENDATIONS

Additional insight into the turbulence processes occurring near the ground could be obtained by additional measurements if two modifications were made to the present experiment: First, expansion of the  $C_T$  measurement system from one pair of fast-response thermal probes to perhaps five pairs spaced 1 m apart; this would allow a determination of the  $C_n^2$  height profile independent of wind and solar-radiation variations. Second, use of larger surfaces would ensure that the differences measured between surfaces are due to the surface under consideration and not to different bordering surfaces and structures.

The results presented indicate a need to repeat the experiment at times of the year having a greater percentage of clear days with higher solar insolation and less wind, such as occur during the summer.

## ACKNOWLEDGMENTS

The author acknowledges the help provided by K. M. Haught in the the development of the computer programs for the data reduction and by M. Woytko, T. Cosden, and C. Gott in the development and operation of the tower system.

## REFERENCES

1. A.N. Kolmogorov, "Dissipation of Energy in Locally Isotropic Turbulence," *Doklady Akad. Nauk SSSR* **32**, 16 (1941).
2. A.M. Obukov, "Structure of the Temperature Field in a Turbulent Flow," *Izvestiya Akad. Nauk SSSR, Seriya Geofizicheskaya* **13**, 58 (1949).
3. L.A. Chernov, *Wave Propagation in a Random Medium*, Dover, New York, 1967.
4. V.I. Tatarskii, *Wave Propagation in a Turbulent Medium*, Dover, New York, 1967.
5. V.I. Tatarskii, *The Effects of the Turbulent Atmosphere on Wave Propagation*, Keter Press, Israel Program for Scientific Translation, Jerusalem, 1971; publication TT 68-50464, U.S. Dept. Commerce, National Technical Information Service, Springfield, VA 22151.
6. G.R. Ochs, R.R. Bergman, and J.R. Snyder, "Laser-Beam Scintillation over Horizontal Paths from 5.5 to 145 Kilometers," *J. Opt. Soc. Am.* **59**, 231 (1969).
7. J.C. Wyngaard, Y. Izumi, and S.A. Collins, Jr., "Behavior of the Refractive-Index-Structure Parameter near the Ground," *J. Opt. Soc. Am.* **61**, 1646 (1971).
8. R.S. Lawrence, G.R. Ochs, and S.F. Clifford, "Measurements of Atmospheric Turbulence Relevant to Optical Propagation," *J. Opt. Soc. Am.* **60**, 826 (1970).
9. J.A. Dowling and P.M. Livingston, "Behavior of focused beams in atmospheric turbulence: Measurements and comments on the theory," *J. Opt. Soc. Am.* **63**, 846 (1973).

10. R.W. Harris, "Optimization of Probe Excitation for a Two-Probe Measurement of the Refractive-Index Structure Function Constant of the Atmosphere," NRL Report 7587, July 31, 1973.